

Evaluation of Pt-Ru-Ir as Bifunctional Electrocatalysts for the Oxygen Electrode in a Unitized Regenerative Fuel Cell

S. Rivas^{1,*}, L. G. Arriaga², L. Morales², A. M. Fernández^{1*}

¹ Centro de Investigación en Energía, Privada Xochicalco S/N Temixco, Morelos C.P. 62580, México

² Centro de Investigación y Desarrollo Tecnológico en Electroquímica S.C., C.P.76703, Querétaro Sanfandila, Qro México

*E-mail: afm@cie.unam.mx

Received: 20 January 2012 / Accepted: 3 March 2012 / Published: 1 April 2012

The Unitized Regenerative Fuel Cell (URFC) is a device that works as a Fuel Cell (FC) to produce electric energy and as a Water Electrolyzer (WE) to produce the oxygen and hydrogen for the FC operation mode. One of the challenges for URFC's is the development of bifunctional electrocatalysts capable of carrying out efficiently the oxygen reduction reaction (ORR) and oxygen evolution reaction (OER), since those electrocatalysts that performs well the oxygen reduction have also poor oxygen evolution performance. The objective of this paper is to evaluate the efficiency of four different atomic composition electrocatalytic materials, based on Pt-Ru-Ir, to carry out the oxygen reduction and evolution reactions. The studies of the performance for this material were made in a Proton Exchange Membrane Fuel Cell (PEMFC), using the linear voltammetry technique at 30, 60 and 80°C in FC and WE mode. The Membrane Electrode Assembly (MEA) was prepared by the Hot-Spray technique for the oxygen electrode without using an electrocatalysts support; meanwhile the hydrogen electrode was prepared using the paste technique over the gas diffusion layer. The electrocatalyst loading was 3-5 mg·cm⁻² on the oxygen electrode and 0.5-1 mg Pt·cm⁻² on the hydrogen side.

Keywords: Oxygen reduction and evolution reactions, Unitized Regenerative Fuel Cells, Bifunctional electrocatalysts.

1. INTRODUCTION

Fuel Cells are one of the most promising technologies for clean energy production. A Fuel Cell (FC) is, in a simple definition, a device that transforms the energy of electrochemical reactions directly in electric energy as long as the corresponding reactive is supplied. There are five basic FC's, classified according to their operating temperature: the Solid Oxide FC (500-1000 °C), the Molten Carbonate FC (~650 °C), the Phosphoric Acid FC (~220 °C), the Alkaline FC (50-200 °C) and the

Proton Exchange Membrane FC (30-100 °C). Among them, the PEMFC has the highest operating range, since they can be designed to supply energy for portable (1-100 W) and domestic (1-100 kW) devices [1]. The PEMFC requires pure hydrogen as fuel and oxygen as oxidant, to produce energy and water plus heat as by-products. Since hydrogen is not naturally available, one of the main challenges for PEMFCs is the development of clean and efficient technologies to produce this fuel. Hydrogen can be produced by reforming fossil fuels although generating pollutants. A cleaner way is by water electrolysis with the advantage of the oxygen production [1,2]. The Solid Polymer Electrolyzer (SPE) has exactly the PEMFC opposite operation reactions, even though its constitution is basically the same. The principal research operation of this device is focused on develop materials that allows to build both systems in one, and it is called the Unitized Regenerative FC (URFC).

A key issue on URFC development is the synthesis of efficient electrocatalysts for oxygen reduction and water electrolysis. Besides, they should be economic and corrosion resistant during electrolysis. Nowadays, platinum is the best electrocatalyst for the oxygen reduction reaction (ORR), but has a poor oxygen evolution performance. Swette *et. al.* [3] studied a different combination of metal/oxide and metal/metal alloys using Pt, Ir, Ru, and Rh metals. They concluded that RuO₂ is better electrocatalyst for WE than IrO₂, however it is unstable for this application. Escalante-García *et al* [4] studied mixtures of IrO₂ with Pt and RuO₂ with Pt supported and unsupported on Ebonex[®]. It is known that metal oxides catalyze the OER but not the ORR, while Pt acts the opposite way, therefore in this work they expected to find an appropriate mixture to achieve an efficient URFC. The supported electrocatalysts displayed a current density fall assigned to a low dispersion capacity of the Ebonex[®]. The supported IrO₂-Pt shows also an OER starting potential displaced compared with the unsupported material. Escalante-García [4] concludes as Swette [3] that RuO₂ performs the OER better than IrO₂ and, although these oxides are not involved in the ORR, nor interfere with the activity of Pt to carry out this reaction.

Another approach studied is using IrO₂ as Pt support [5], the results are affected by particle size, besides a higher performance has been achieved when the electrocatalysts is deposited on the support since it has a better distribution than a physical mixture [6]. Chen *et. al.* [7] worked with combinatorial chemistry to evaluate 715 combinations of Pt, Ru, Os, Ir and Rh. They identified Pt_{4.5}Ru₄Ir_{0.5} as the most efficient electrocatalyst for URFC, they also concluded that the addition of Ru increases reaction rate. According with Sung-Dae Yim *et. al.* [8] studies, the oxides or metals of Pt, Ir and Ru were best electrocatalyst for URFC; in particular the following ratio PtIr (50/50), while adding Ruthenium has a positive effect only for WE.

This work presents the evaluation in a PEMFC of four unsupported different atomic compositions of Pt-Ru-Ir as bifunctional electrocatalyst for a URFC.

2. EXPERIMENTAL

2.1. Electrocatalysts Synthesis

The ternary material Pt-Ru-Ir was synthesized using H₂PtCl₆*H₂O (Fluka[®]), RuCl₃ (Aldrich[®]) y IrBr₃ (Aldrich[®]) diluted in deionized water (Millipore 18MΩ) at 10mM concentration. A 40-fold molar

excess of 5% aqueous NaBH_4 (Fermont 98%) was used as reducing agent. Adding NaBH_4 allowed a faster product precipitation. The precipitate was filter and washed with deionized water and dried at 80°C on air. The synthesized electrocatalysts are: $\text{Pt}_x\text{Ru}_y\text{Ir}_z$, $\text{Pt}_{(x-1)}\text{Ru}_y\text{Ir}_{(z+1)}$, $\text{Pt}_{(x-2)}\text{Ru}_y\text{Ir}_{(z+2)}$ and $\text{Pt}_{(x-3)}\text{Ru}_y\text{Ir}_{(z+3)}$, where $x = 4.5$, $y = 4$ and $z = 0.5$. Every metal was also synthesized using the same method in order to test a ternary mixture and PtIr (85/15 w %).

2.2 Electrocatalyst characterization

The structure of the electrocatalysts was analyzed by X- Ray Diffraction using a Rigaku diffractometer D/MAX-2200 with a $\text{CuK}\alpha$ (0.154059. nm) anode. The samples were scanned from 20° to 100° at $0.08^\circ/\text{min}$. The phase structure was compared with the X-ray diffraction patterns Joint Committee on Power Diffraction Standards (JCPDS) of every elemental material. Software Jade 6.5 was used to estimate the average grain size of samples. The morphology of Pt-Ru-Ir was examined using a JEOL JSM5335 Scanning Electron Microscope.

2.3 Membrane Electrode Assembly (MEA) manufacturing

The oxygen electrode was made applying the electrocatalyst on Nafion[®] 115 membrane using the Hot-Spray technique. The hydrogen electrode was prepared by deposition of the electrocatalyst on the diffuser (E-TEK, PEMEAS, Boston, USA) using the paste technique. The synthesized electrocatalyst was dispersed in Nafion[®] solution (5% wt, Aldrich) by means of ultrasonic bath until evaporate the ionomer solvent. The powder was triturated in order to get a smaller particle size, and after that it was dispersed on propanol solution and then sprayed over the membrane. The hydrogen electrode was fabricated with Pt 30% wt supported on Vulcan XC-72. Finally, the MEA were pressed at $400\text{ kg}\cdot\text{cm}^{-2}$ and the temperature was 120°C , during 90 seconds. The electrocatalyst loading on the oxygen electrode was $3\text{-}5\text{ mg}\cdot\text{cm}^{-2}$ and $0.5\text{-}1\text{ mg Pt}\cdot\text{cm}^{-2}$ on the hydrogen side. Both electrodes were prepared using a weight rate of 33% Nafion[®] and 67% electrocatalyst.

2.4 Evaluation as URFC

For the FC operation mode pure oxygen (Praxair[®] 4.3 UHP) and hydrogen (Praxair[®] research grade) gases were used. The operating conditions were: the gases pressure was $2.11\text{ kg}\cdot\text{cm}^{-2}$ (30 psi) and oxygen and hydrogen flows were $0.100\text{ L}\cdot\text{min}^{-1}$ and $0.050\text{ L}\cdot\text{min}^{-1}$ respectively. For the WE operation mode, a continuous deionized water flow ($0.005\text{ L}\cdot\text{min}^{-1}$) was supplied to the oxygen side. The evaluation hardware is a 5 cm^2 FC, the cell was connect to a PS-CompuCell and PSDM Electrochem test stations operate with a PGSTAT 302 potentiostat with a Booster 20A, both of Autolab Company.

The evaluation test consisted in obtaining the polarization curves for the FC mode scanning from the open circuit potential (OCP) until 0.25 V at $10\text{ mV}\cdot\text{s}^{-1}$ sweep rate, for the WE mode linear voltammetry was measured from 0.8 V to 1.8 V at $50\text{ mV}\cdot\text{s}^{-1}$. Electrochemical impedance

spectroscopy was used to measure the ohmic resistance in a frequency range of 10 kHz-10 Hz and the ac signal amplitude of 10 mV was used. Every test was conducted at different temperature (30, 60 and 80 °C) on both, gases and cell.

In order to determine if the WE operation mode has any effect on the performance of FC, the evaluation sequence was PEMFC-WE-PEMFC2-WE2.

3. RESULTS AND DISCUSSION

3.1. Electrocatalyst characterization

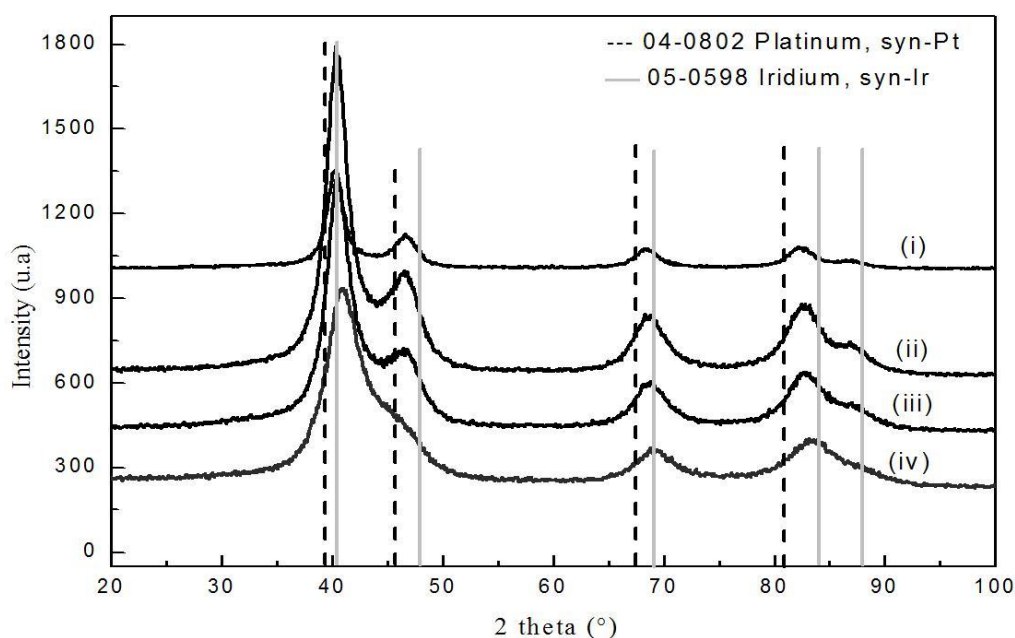


Figure 1. X-ray diffraction patterns of (i) $Pt_xRu_yIr_z$, (ii) $Pt_{x-1}Ru_yIr_{z+1}$, (iii) $Pt_{x-2}Ru_yIr_{z+2}$, and (iv) $Pt_{x-3}Ru_yIr_{z+3}$.

The X-Ray pattern is shown on Figure 1. We can observe from this graph that if the amount of Ir decreases, the diffraction peaks become wider and less intense; it is the opposite behavior when the Pt amount increases. When the Pt-Ru-Ir diffractograms are compared with the individual diffractogram of Ir, Pt and Ru, it cannot be distinguished those phases in the ternary material. The diffraction peaks of the electrocatalyst are shifted to the right side, this is an indication of the alloy formation between Pt and Ir, however Ru couldn't be identified by this technique. This is because during the synthesis of the electrocatalyst, the Ru resulted with an amorphous structure. According to this displacement of the diffraction peaks it is possible to mention that there is a formation of the solid solution created by substitution between Pt and Ir. The average crystal size was 9 nm for the synthesized material in its different compositions. Tsutomu *et. al.* [9] reported a formation of PtIr alloy by the shifting of the diffraction peaks. Min-Soon *et.al.*[10] prepared PtRu/C electrocatalyst varying

the NaBH_4 concentration; the results are similar to those shown in Figure 1. Kim *et. al.* [11] assigned the second's peaks fall intensity to an increment of Ru content from 30 to 60 % atomic.

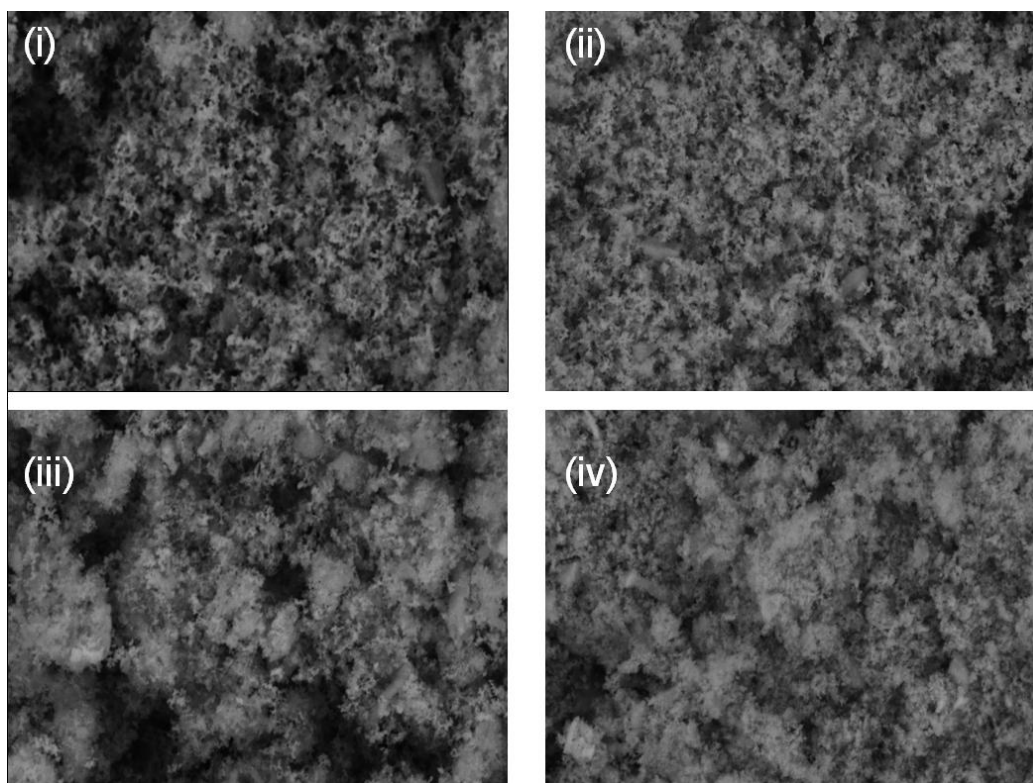


Figure 2. Scanning Electron Micrograph of (i) $\text{Pt}_x\text{Ru}_y\text{Ir}_z$, (ii) $\text{Pt}_{x-1}\text{Ru}_y\text{Ir}_{z+1}$, (iii) $\text{Pt}_{x-2}\text{Ru}_y\text{Ir}_{z+2}$, and (iv) $\text{Pt}_{x-3}\text{Ru}_y\text{Ir}_{z+3}$ electrocatalysts. 25.00KX.

The XRD diffraction pattern of Pt_xIr_z synthesized and of the Pt-Ir (85/15 %) mixture did not shown any displacement of their peaks. As a consequence of this observation it is possible to mention that the presence of Ru help to produce a solid solution between Pt and Ir.

Figure 2 shows the microstructure of the electrocatalysts materials. In this figure it is possible to observer that the electrocatalyst with less Platinum (Figure 2(iv)) has two type of formation, one looks more dense and distributed in the entire sample, and over this one, there is another more compact. However, when the electrocatalyst has more Platinum the morphology looks like “cauliflower” form (Figure 2 (i)).

3.2 Evaluation as URFC

Figure 3 shows the performance of the electrocatalyst materials on FC mode, before and after the WE. From the figure it can be observed a decrease in the current density for electrocatalytic materials. In such materials, from (ii) to (iv), the Pt amount was reduced.

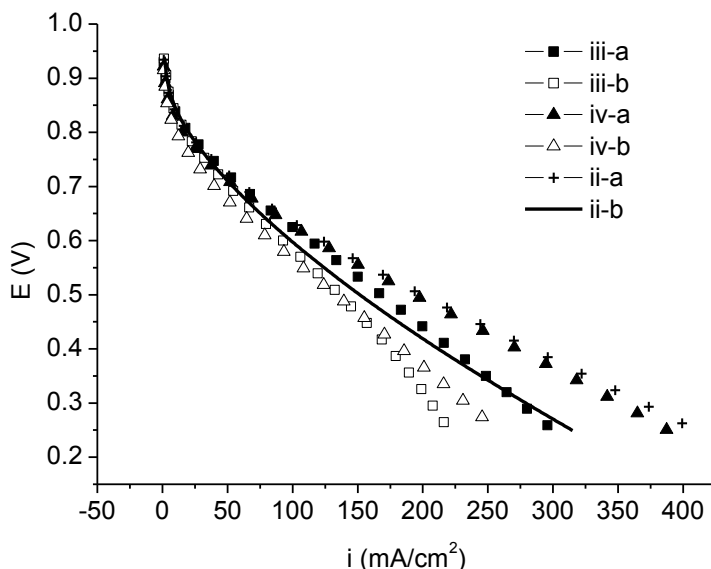


Figure 3. Evaluation of ternary material in to PEMFC with a $T_{cell} = T_{gases} = 80\text{ }^{\circ}\text{C}$, $P_{H_2} = P_{O_2} = 30\text{ psi}$, flow $O_2/H_2 = 100/50\text{ ml/min}$. FC mode before and after the WE. [(ii) $Pt_{x-1}Ru_yIr_{z+1}$, (iii) $Pt_{x-2}Ru_yIr_{z+2}$, (iv) $Pt_{x-3}Ru_yIr_{z+3}$, “a and b” means before and after WE test.

The internal ohmic resistance of the cell was determined with impedance spectroscopy at OCP on FC mode, the resistance can be read on Z' where $Z'' = 0$ at high frequency. The Tafel slope can be determined with the E vs $\log(i)$ plot.

Table I shows the Tafel slope and resistance corresponding to the electrocatalyst materials in FC mode, before and after the WE operation.

Table I. Fuel Cell resistance and Tafel slope before and after the WE operation mode.

Material	b_{pre-E} (mV/dec)	R_{pre-E} ($\Omega\text{-cm}^2$)	b_{post-E} (mV/dec)	R_{post-E} ($\Omega\text{-cm}^2$)
$Pt_xRu_yIr_z$	169.4	0.3443	160	0.2953
$Pt_{(x-2)}Ru_yIr_{(z+2)}$	108.2	0.352	139	0.4522
$Pt_{(x-3)}Ru_yIr_{(z+3)}$	106.1	0.37693	128	0.4253
$Pt_{(x-1)}Ru_yIr_{(z+1)}$	110.8	0.43572	134	0.83605
$Pt_{85}Ir_{15}$	126.9	0.216375	127	0.20485

Both parameters increase after the WE process, only the electrocatalyst with the following ratio $Pt_{85}Ir_{15}$ keeps a steady performance. Before the WE mode the FC power density at 0.65V was $60\text{ mW}\cdot\text{cm}^{-2}$ for the Pt-Ru-Ir electrocatalysts, while $Pt_{85}Ir_{15}$ has $80\text{ mW}\cdot\text{cm}^{-2}$. After the WE the power density of those with Ru falls to $40\text{-}55\text{ mW}\cdot\text{cm}^{-2}$, while binary material stays at $80\text{ mW}\cdot\text{cm}^{-2}$.

This behavior is related to the URFC system stability, similar results have been reported by Sung-Dae Yim [8] for PtIr (50:50) and by S. Zhigang [12], and Ho-Young Jung [13] reports a stable behavior for the $Pt_{85}Ir_{15}$ during 120 hours at $500\text{ mA}\cdot\text{cm}^{-2}$ making cycles of 10 and 20 hours on FC and WE mode respectively. According to Zhigang [12] this performance fall is caused by water

accumulation in the diffuser pores during the WE operation mode, however, it reaches a stable performance after the third URFC cycle. In contrast, during the experiments shown in this work, the fuel cell was N₂ purged before switching from one operation mode to another, therefore we cannot assign the performance fall only to a mass transfer problem due to water accumulation in the gas diffuser.

Table II. Efficiency for WE operation mode ($\epsilon = 1.48/E_{WE} = \Delta h_f/nFE_{WE}$).

Material	E _{WE}	Efficiency
Pt _x Ru _y Ir _z	1.736	86.04
Pt _(x-2) Ru _y Ir _(z+2)	1.6865	88.56
Pt _(x-3) Ru _y Ir _(z+3)	1.6929	88.23
Pt _(x-1) Ru _y Ir _(z+1)	1.725	86.59
Pt ₈₅ Ir ₁₅	1.7	87.86

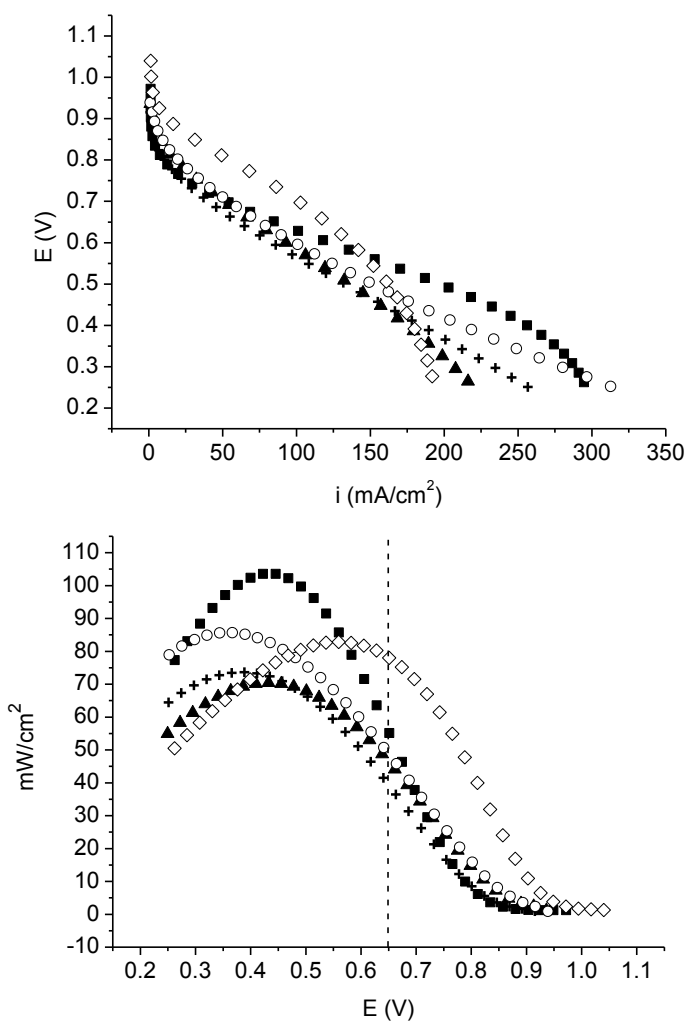


Figure 4. FC polarization and power curves post WE test. T_{cell} = T_{gases} = 80 °C, P_{H2} = P_{O2} = 30
 [■Pt_xRu_yIr_z, ▲Pt_(x-2)Ru_yIr_(z+2), +Pt_(x-3)Ru_yIr_(z-3), ○Pt_(x-1)Ru_yIr_(z+1), ◇Pt₈₅Ir₁₅].

The polarization and power curves for FC after the WE test are presented in Figure 4. The Tafel slopes determined at the low current density zone are higher in contrast to the reported values ($60 \text{ mV} \cdot \text{dec}^{-1}$ – $120 \text{ mV} \cdot \text{dec}^{-1}$ for Pt), the cell resistance is also high (see Table I).

Even though the FC with $\text{Pt}_x\text{Ru}_y\text{Ir}_z$ as electrocatalyst produced higher power than the one with $\text{Pt}_{85}\text{Ir}_{15}$, it is at a lower potential than the practical value for FC operation (0.65 V/cell)

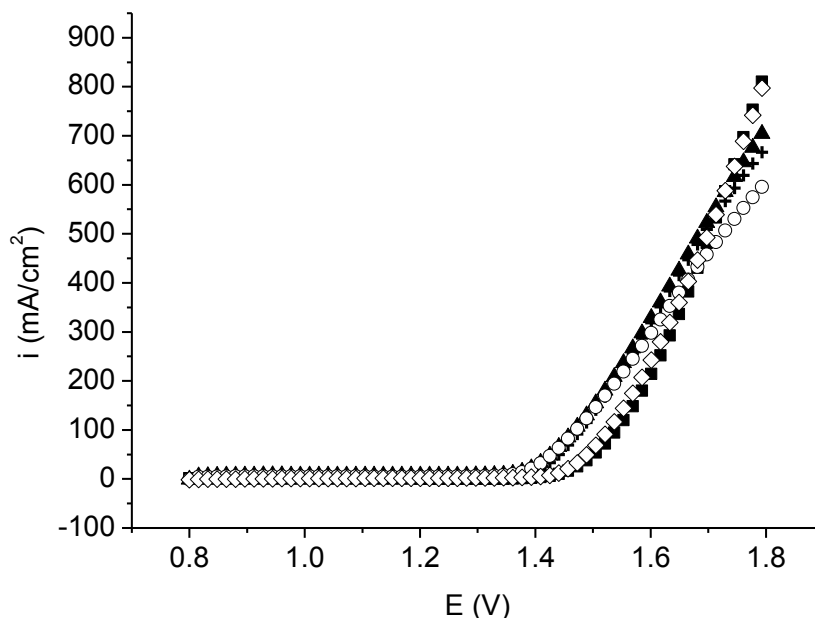


Figure 5. Electrolysis test, water flow = 5 ml H_2O /min. $T_{\text{cell}} = T_{\text{water}} = 80 \text{ }^\circ\text{C}$. [\blacksquare $\text{Pt}_x\text{Ru}_y\text{Ir}_z$, \blacktriangle $\text{Pt}_{(x-2)}\text{Ru}_y\text{Ir}_{(z+2)}$, $+$ $\text{Pt}_{(x-3)}\text{Ru}_y\text{Ir}_{(z-3)}$, \circ $\text{Pt}_{(x-1)}\text{Ru}_y\text{Ir}_{(z+1)}$, \diamond $\text{Pt}_{85}\text{Ir}_{15}$].

The WE curves are shown on figure 5, the $\text{Pt}_{85}\text{Ir}_{15}$ electrocatalyst has a stable performance, and most of the ternary materials had a performance improvement, except for the $\text{Pt}_x\text{Ru}_y\text{Ir}_z$ electrocatalyst.

According to the WE performance, it seems that adding Ru has slight effect, being more relevant the Pt/Ir composition. The mix $\text{Pt}_{85}\text{Ir}_{15}$ and $\text{Pt}_x\text{Ru}_y\text{Ir}_z$ were, among the tested materials, the best electrocatalysts for WE, producing higher current density, yet only the binary material has a stable performance in a URFC system. Table II shows the efficiency values calculated at $500 \text{ mA} \cdot \text{cm}^{-2}$. However, current efficiency was not considered, because not all the applied current is used to produce gases.

According to the E-pH diagrams, it is likely the formation of IrO_2 at the potential values where a WE works. Ruthenium, just like Osmium is the less noble on Platinum group, therefore it can be corroded at 1.4-1.5 V at acid pH (0-2) [14-15], in this conditions the formation of RuO_4 gas is possible. All this would explained the performance fall on FC mode, since these oxides are efficient for WE, but not for the Oxygen Reducing Reaction (ORR).

In general terms and considering the URFC operation, the $\text{Pt}_{85}\text{Ir}_{15}$ electrocatalyst has a better behavior than the ternary material synthesized for this work, not only due to its efficiency but its stability.

4. CONCLUSIONS

Research on electrocatalyst development has to consider not only efficiency and cost, but the electrocatalyst stability under the operating conditions of interest. During this study we were able to evaluate both aspects of the synthesized electrocatalysts. The results presented here indicate that the ternary materials synthesized are unstable for URFC conditions. According to the X-Ray Diffraction, it might be present a PtIr alloy, but there is not enough information to conclude about the Ru state in the PtIr alloy. It could also be possible that not all the Ir is alloyed to the Pt and therefore an Ir oxide might be formed during the electrolysis process.

ACKNOWLEDGEMENTS

This work was partially supported by DGAPA-UNAM under the postdoctoral program and the PAPIIT-DGAPA-UNAM project IN109609. We wish to thank Maria Luisa Ramon Garcia of CIE-UNAM for the XRD measurement.

References

1. J. Larminie J, A. Dicks. *Fuel Cell Systems Explained*. 2nd ed. John Wiley & Sons Ltd. England (2003).
2. Wells Fargo Special Report. Identifying the Opportunities in Alternative Energy. Available in: https://www.wellsfargo.com/downloads/pdf/about/csr/alt_energy.pdf.
3. L. Swette, A. LaConti, S. A. McCatty, *J. Power Sources*, 47 (1994) 343.
4. I. L. Escalante-García, S.M. Duron-Torres, J. C. Cruz, L. G. Arriaga-Hurtado. *J. New Mat. Electrochem. Systems* 13 (2010) 227.
5. W. Yao, J. Yang, J. Wang, Y. Nuli. *Electrochem. Commun.* 9 (2007) 1029.
6. T. Ioroi, N. Kitazawa, K. Yasuda, Y. Yamamoto, H. Takenaka. *J Appl. Electrochem.* 31 (2001) 1179.
7. G. Chen, D. A. Delafuente, S. Sarangapani, T. E. Mallouk, *Catal. Today* 67 (2001) 341.
8. S-D Yim, W-Y Lee, Y-G Yoon, Y-J Sohn, G-G Park, Y-H Yang, C-S Kim. *Electrochim. Acta* 50 (2004) 713.
9. T. Ioroi, K Yasuda. *J Electrochemical Soc.* 152 (2005) A1917.
10. M-S Hyun, S-K Kim, B Lee, D Peck, Y Shul, D Jung. *Catal. Today* 132 (2008) 138.
11. T-W Kim, S-J Park, L. E. Jones, M. F. Toney, K-W Park, Y-E Sung. *J. Phys. Chem. B*, 109 (2005) 12845.
12. S Zhigang, Y Baolian, H Ming, *J. Power Sources*, 79 (1999) 82.
13. H-Y Jung, S Park, B. N Popov. *J. Power Sources*, 191 (2009) 357.
14. M. J. N. Pourbaix, J. V. Muylder, N. Zoubov. *Platinum Metals Rev.*, 3 (1959) 100.
15. Encyclopedia of Electrochemistry of the Elements. Vol 5. Marcel Dekker, Inc., New York (1976).